Sequential Displacement of Coordinated Ethene by Hexafluorobenzene: Crystal Structures of η^2- and η^4-Hexafluorobenzene Complexes of Iridium

Tanachat W. Bell,[1a] Madeleine Helliwell,[1b] Martin G. Partridge,[1a] and Robin N. Perutz*,[1a]

Departments of Chemistry, University of York, York YO1 5DD, U.K., and University of Manchester, Manchester M13 9PL, U.K.

Received November 5, 1991

The photochemical reaction of $(\eta^5\text{-}C_5R_5)Ir(C_2H_4)_2$ (R = H, Me) with hexafluorobenzene effects sequential replacement of coordinated ethene by hexafluorobenzene, yielding $(\eta^5\text{-}C_5R_5)Ir(C_2H_4)(\eta^2\text{-}C_6F_6)$ followed by $(\eta^5\text{-}C_5R_5)Ir(\eta^4\text{-}C_6F_6)$. The first product, $(\eta^5\text{-}C_5R_5)Ir(C_2H_4)(\eta^2\text{-}C_6F_6)$, is present in solution as two isomers which interconvert slowly compared with the NMR relaxation time, T_1. The dominant isomer of $(\eta^5\text{-}C_5H_5)Ir(C_2H_4)(\eta^2\text{-}C_6F_6)$ exhibits coupling between ethene nuclei and ^{19}F, suggestive of a C–H···F interaction. The minor isomer is postulated to be related to the major isomer by 180° rotation about the vector joining Ir to the midpoint of the coordinated C–C bond of C_6F_6. All the complexes exhibit three mutually coupled resonances in the ^{19}F NMR spectrum, indicating that the C_6F_6 units are stereochemically rigid. The X-ray crystal structure of $(\eta^5\text{-}C_5H_5)Ir(C_2H_4)(\eta^2\text{-}C_6F_6)$ (a = 7.784 (3) Å, b = 12.642 (5) Å, c = 14.728 (4) Å, β = 119.98 (2)°, monoclinic, space group $P2_1/c$, Z = 4, no crystallographically imposed symmetry) reveals a typical half-sandwich geometry of the type $(\eta^5\text{-}C_5H_5)Ir(L)L'$. The C_6F_6 ligand is bound through two carbons (mean r(Ir–C) = 2.08 (2) Å) and distorted so as to generate a planar C_6F_4 unit with the remaining two fluorines bent out of plane (dihedral angle 47.9°) and in very close contact with the coordinated ethene (r(C(1)···F(4) = 2.87 (2) Å). The C_6F_4 moiety has a "diene-coordinated ene" distortion of the C–C distances, which range from 1.34 (3) Å in the uncoordinated diene unit to 1.47 (2) Å for the coordinated C–C bond. The structure of $(\eta^5\text{-}C_5H_5)Ir(\eta^4\text{-}C_6F_6)$ (a = 5.950 (3) Å, b = 11.592 (3) Å, c = 15.122 (3) Å, orthorhombic, space group *Pnma*, Z = 4, crystallographically imposed mirror plane bisecting the C_6F_6 ligand) shows the C_6F_6 ligand coordinated through four carbons essentially equidistant from iridium (2.09 (1) and 2.10 (1) Å). The C_6F_6 ring is strongly bent into a structure like an open book with two carbons tilted away from the metal (dihedral angle between the ring planes is 135.5°). The C–C distances of the ring are distorted to a "ene-coordinated diene" arrangement with values for the coordinated carbons of 1.41 (2) and 1.44 (2) Å, while the uncoordinated double bond is significantly shorter at 1.29 (3) Å.

Introduction

It was established many years ago that C_2F_4 coordinates strongly to transition-metal centers and that electron-withdrawing substituents often stabilize metal–alkene complexes (consider for instance, $CpRh(C_2H_4)(C_2F_4)$, Cp = $\eta^5\text{-}C_5H_5$).[2] In contrast, η^6-arene complexes, such as $Cr(\eta^6\text{-}C_6H_6)_2$, undergo arene exchange more readily with electron-withdrawing groups on the arene.[3] In the 1960s and 1970s it was also discovered that hexakis(trifluoromethyl)benzene can function as a two-electron (η^2) or a four-electron (η^4) donor in such complexes as $Pt(PEt_3)_2[\eta^2\text{-}C_6(CF_3)_6]$ and $CpRh[\eta^4\text{-}C_6(CF_3)_6]$.[4,5] The $C_6(CF_3)_6$ ligand is highly distorted in these complexes, so that it behaves as a coordinated polyene. However, the stability of these complexes does not seem to have been linked to the stabilizing role of electron-withdrawing substituents for alkene complexes. Recently, we demonstrated that oxidative addition of arenes could be arrested at the η^2 stage if benzene is replaced by hexafluorobenzene. Thus, $CpRh(PMe_3)(C_2H_4)$ reacts photochemically with benzene to yield $CpRh(PMe_3)(Ph)H$ but reacts with hexafluorobenzene to form isolable $CpRh(PMe_3)(\eta^2\text{-}C_6F_6)$.[6] The corresponding pentamethylcyclopentadienyl complex reacts similarly in the first stage but proceeds to activate a carbon–fluorine bond on prolonged irradiation, forming $Cp^*Rh(PMe_3)(C_6F_5)F$.[7a] The analogy between $\eta^2\text{-}C_6(CF_3)_6$ and $\eta^2\text{-}C_6F_6$ as ligands was evident, as was the role of the fluorine atoms in stabilizing the complexes. A further indication of the ability of highly electron-withdrawing groups to stabilize η^2-arene complexes came with the demonstration that $CpRh(PMe_3)(C_2H_4)$ reacts photochemically with $1,4\text{-}C_6H_4(CF_3)_2$ to form an equilibrium mixture of η^2-arene and aryl hydride complexes.[7b]

We were interested in investigating the effect of metal and ancillary ligands on the reactions of hexafluorobenzene. In this paper, we show that $(\eta^5\text{-}C_5R_5)Ir(C_2H_4)_2$ (R = H, Me) reacts photochemically with C_6F_6 in two steps to displace first one ethene and then another, yielding $\eta^2\text{-}C_6F_6$ and $\eta^4\text{-}C_6F_6$ complexes.

Experimental Section

Synthetic Methods. The syntheses were carried out with standard Schlenk methods under an argon atmosphere. Solutions were irradiated with an Applied Photophysics 250-W high-pressure mercury arc in small Pyrex ampules fitted with a PTFE stopcock. Hexafluorobenzene (99%) from Aldrich was distilled under argon and stored over molecular sieves (grade 4a) prior to use. Deuterated solvents were obtained from Goss and dried over potassium benzophenone ketyl. Microanalyses were performed by Leeds University Chemistry Department Analytical Service.

* To whom correspondence should be addressed.

(1) (a) University of York. (b) University of Manchester.

(2) Guggenberger, L. J.; Cramer, R. *J. Am. Chem. Soc.* **1972**, *94*, 3799. Mingos, D. M. P. In *Comprehensive Organometallic Chemistry*; Wilkinson, G., Stone, F. G. A., Abel, E. W., Eds.; Pergamon Press: Oxford, U.K., 1982; Vol. 3, p 1, and references therein.

(3) Muetterties, E. L.; Bleeke, J. R.; Sievert, A. C. *J. Organomet. Chem.* **1979**, *178*, 197. Zimmerman, C. L.; Shaner, S. L.; Roth, S. A.; Willeford, B. R. *J. Chem. Res., Synop.* **1980**, 108.

(4) Browning, J.; Green, M.; Penfold, B. R.; Spencer, J. L.; Stone, F. G. A. *J. Chem. Soc., Chem. Commun.* **1973**, 31. Browning, J.; Penfold, B. R. *J. Cryst. Mol. Struct.* **1974**, *4*, 335.

(5) Churchill, M. R.; Mason, R. *Proc. R. Soc. London, Ser. A* **1966**, *292*, 61.

(6) Belt, S. T.; Duckett, S. B.; Helliwell, M.; Perutz, R. N. *J. Chem. Soc., Chem. Commun.* **1989**, 928.

(7) (a) Jones, W. D.; Partridge, M. G.; Perutz, R. N. *J. Chem. Soc., Chem. Commun.* **1991**, 264. (b) Belt, S. T.; Dong, L.; Duckett, S. B.; Jones, W. D.; Partridge, M. G.; Perutz, R. N. *J. Chem. Soc., Chem. Commun.* **1991**, 266.

0276-7333/92/2311-1911$03.00/0

Table I. NMR Parameters for C_6F_6 Complexes in Toluene-d_8

^{1}H			^{19}F		^{13}C{^{1}H}	
δ/ppm	integral	assignt	δ/ppm	assignt[b]	δ/ppm	assignt
			$CpIr(C_2H_4)(\eta^2\text{-}C_6F_6)$ (Major Isomer)			
4.20 (s)	5	C_5H_5	−146.8 (m)	F(5)	88.6 (s)	C_5H_5
2.72 (m)[c]	2	C_2H_4	−172.4 (m)	F(6)	28.6 (d, J_{CF} = 16.5 Hz)	C_2H_4
2.30 (m)[c]	2	C_2H_4	−179.1 (m)	F(4)		
			$CpIr(C_2H_4)(\eta^2\text{-}C_6F_6)$ (Minor Isomer)			
4.72 (s)		C_5H_5	−147.1 (m)	F(5)	88.4 (s)	C_5H_5
2.46 (m)		C_2H_4	−150.2 (m)	F(4)	28.8 (s)	C_2H_4
0.24 (m)		C_2H_4	−171.7 (m)	F(6)		
			$CpIr(\eta^4\text{-}C_6F_6)$			
4.56 (s)		C_5H_5	−141.9 (m)			
			−181.7 (m)	F bound to coordinated C		
			−189.1 (m)	F bound to coordinated C		
			$Cp^*Ir(C_2H_4)(\eta^2\text{-}C_6F_6)$ (Isomer 1)			
1.50 (s)	15	C_5Me_5	−147.7 (m)	F(5)		
2.73 (m)		C_2H_4[a]	−170.7 (m)	F(4)	37.3 (d, J_{CF} = 20 Hz)	C_2H_4[a]
			−173.3 (m)	F(6)		
			$Cp^*Ir(C_2H_4)(\eta^2\text{-}C_6F_6)$ (Isomer 2)			
1.17 (s)	15	C_5Me_5	−145.7 (m)	F(5)		
0.73 (m)		C_2H_4[a]	−176.2 (m)	F(6)	38.7 (s)	C_2H_4[a]
			−177.9 (m)	F(4)		
			$Cp^*Ir(\eta^4\text{-}C_6F_6)$			
1.61 (s)	15	C_5Me_5	−141.6 (m)			
			−187.2 (m)	F bound to coordinated C		
			−202.9 (m)	F bound to coordinated C		

[a] Uncertain as to which isomer this resonance belongs. No attempt was made to purify $Cp^*Ir(C_2H_4)(\eta^2\text{-}C_6F_6)$, and not all ethene resonances were located. [b] Numbering of fluorines as in Figures 2 and 4. [c] Coupling constants (Hz) used in the simulation were as follows (numbering refers to diagram A in the text; in each case one set out of the symmetry-related pair of coupling constants is listed): HH couplings $J(1,6)$ = 12.18, $J(1,2)$ = $J(5,6)$ = 8.8, $J(1,5)$ = −0.67; FF coupling $J(3,4)$ = 24; HF couplings $J(1,3)$ = 1.75, $J(3,5)$ = 0.95, $J(4,5)$ = 0.6. The simulation was performed with 16K data points and a line width of 0.55 Hz.

Spectroscopic Methods. NMR spectra were measured on a Bruker MSL 300 instrument in toluene-d_8 referenced as follows: ^{1}H relative to C_7D_7H at δ 2.10, ^{13}C relative to C_7D_8 at δ 21.3, ^{19}F relative to external CCl_3F. ^{13}C{^{1}H} NMR spectra were recorded with and without a DEPT pulse sequence. Integrations of proton resonances of the Cp complexes were recorded with a 25° pulse angle and a single pulse to avoid problems caused by slow relaxation. ^{1}H{^{19}F} spectra were measured on a Bruker AMX 250 instrument. NMR spectra were simulated with the aid of the PANIC software on the Bruker MSL 300 spectrometer. Mass spectra were recorded on a Kratos MS3074 or on a VG Autospec instrument. Infrared spectra were measured on a Mattson Sirius FTIR spectrometer.

Synthesis of $CpIr(C_2H_4)(\eta^2\text{-}C_6F_6)$ and $CpIr(\eta^4\text{-}C_6F_6)$. $CpIr(C_2H_4)_2$ (50 mg, 1.6×10^{-4} mol), synthesized as described previously,[8a,b] was dissolved in 15 cm^3 of C_6F_6 and irradiated with a λ > 315 nm cutoff filter for 16 h in a small photoreactor (volume 15 cm^3) with Schlenk connections designed to fit over an Applied Photophysics (100 W) immersion mercury arc like a sleeve. The solution turned brown and also formed some brown precipitate. The solvent was removed in vacuo and the residue sublimed at 70 °C (10^{-3} mbar). The sublimate was further purified by column chromatography on silica (40% Et_2O, 60% hexane). Following removal of the solvent, the two products were separated by fractional sublimation. Pale yellow $CpIr(\eta^4\text{-}C_6F_6)$ sublimes at 30 °C (10^{-1} mbar), while the yellow $CpIr(C_2H_4)(\eta^2\text{-}C_6F_6)$ sublimes at 45–50 °C (10^{-1} mbar). The products were recrystallized from hexane (−20 °C). NMR spectra are listed in Table I. Anal. Calcd for $CpIr(C_2H_4)(\eta^2\text{-}C_6F_6)$ ($C_{13}H_9F_6Ir$): C, 33.12; H, 1.92. Found: C, 33.5; H, 1.9. Mass spectrum for $CpIr(C_2H_4)(\eta^2\text{-}C_6F_6)$: m/z for ^{193}Ir 472 (0.6%, M^+), 444 (0.4%, $M^+ - C_2H_4$), 425 (0.8%, $M^+ - C_2H_4F$), 286 (45%, $M^+ - C_6F_6$), 284 (100%, $M^+ - C_6F_6H_2$), 258 (35%, $CpIr^+$), 186 (19%, $C_6F_6^+$). Infrared spectrum (ν, cm^{-1}; 2000–550-cm^{-1} region) for $CpIr(C_2H_4)(\eta^2\text{-}C_6F_6)$: 1705 m, 1627 w, 1424 m, 1328 m, 1313 w, 1248 m, 1188 w, 1090 w, 951 m, 925 m, 830 w, 697 m, 593 w. Mass spectrum for $CpIr(\eta^4\text{-}C_6F_6)$: m/z for ^{193}Ir 444 (75%, M^+), 277 (53%, $M^+ - C_6F_5$), 258 (100%, $CpIr^+$), 232 (20%), 230 (25%).

Synthesis of $Cp^*Ir(\eta^4\text{-}C_6F_6)$. Hexafluorobenzene (3 cm^3) was condensed into an ampule fitted with a PTFE stopcock containing 25 mg (6.5×10^{-5} mol) of $Cp^*Ir(C_2H_4)_2$, synthesized by literature methods[8c] from $[Cp^*Ir(\mu\text{-}Cl)Cl]_2$.[8d] The sample was irradiated for 23 h (λ > 290 nm), causing the solution to change from colorless to yellow. After removal of the solvent in vacuo, the residue was extracted with 5 cm^3 of hexane to give a pale yellow solution. The solution was pumped to dryness and the residue sublimed onto a liquid-nitrogen-cooled finger (35 °C, 4×10^{-4} mbar). The sublimate was recrystallized from hexane, yielding pure $Cp^*Ir(\eta^4\text{-}C_6F_6)$. NMR data are listed in Table I. Mass spectrum for $Cp^*Ir(\eta^4\text{-}C_6F_6)$: m/z for ^{193}Ir 514 (81%, M^+), 347 (71%, $M^+ - C_6F_5$), 324 (100%). Infrared spectrum (ν, cm^{-1}; 2000–550-cm^{-1} region): 1692 w, 1469 w, 1384 w, 1329 w, 1304 w, 1269 w, 1193 w, 1027 w, 913 m, 570 w.

Crystal Structure of $CpIr(C_2H_4)(\eta^2\text{-}C_6F_6)$. The structure of $CpIr(C_2H_4)(\eta^2\text{-}C_6F_6)$ was determined on a Nicolet R3m/V diffractometer with graphite-monochromated Mo Kα radiation.[9,10] Lattice parameters and an orientation matrix were determined by a least-squares refinement of 25 centered reflections found in a random search (range $11.4 < 2\theta < 25.5°$). Conditions for data collection and reduction are contained in Table II. An empirical absorption correction based on azimuthal scans of three reflections was applied, resulting in transmission factors ranging from 0.74 to 1. The iridium atom was located with the Patterson method. A difference Fourier map then revealed the positions of the other nonhydrogen atoms. The cyclopentadienyl ring was treated as a rigid pentagon with C–C distances of 1.420 Å. All non-hydrogen

(8) (a) Bell, T. W.; Haddleton, D. M.; McCamley, A.; Partridge, M. G.; Perutz, R. N.; Willner, H. *J. Am. Chem. Soc.* **1990**, *112*, 9212. (b) Mayer, J. M.; Calabrese, J. C. *Organometallics* **1984**, *3*, 1292. (c) Moseley, K.; Kang, J. W.; Maitlis, P. M. *J. Chem. Soc. A* **1970**, 2875. (d) Kang, J. W.; Moseley, K.; Maitlis, P. M. *J. Am. Chem. Soc.* **1969**, *91*, 5970.

(9) (a) Sheldrick, G. M. SHELXTL-Plus, release 3.4; Nicolet XRD Corp.: Madison, WI, 1987. (b) Molecular Structure Corporation TEXSAN Structure Analysis Package; Molecular Structure Corp.: College Station, TX, 1985.

(10) Cromer, D. T. *International Tables for Crystallography*; Kynoch Press: Birmingham, U.K., 1974; Vol. IV. (b) Ibers, J. A.; Hamilton, W. C. *Acta Crystallogr.* **1964**, *17*, 781.

Table II. Crystallographic Parameters for Structures of $CpIr(C_2H_4)(\eta^2\text{-}C_6F_6)$ and $CpIr(\eta^4\text{-}C_6F_6)$

	$CpIr(C_2H_4)(\eta^2\text{-}C_6F_6)$	$CpIr(\eta^4\text{-}C_6F_6)$
empirical formula	$C_{13}H_9F_6Ir$	$C_{11}H_5F_6Ir$
color and habit	yellow block	yellow block
cryst size/mm	0.2 × 0.2 × 0.15	0.15 × 0.05 × 0.15
cryst syst	monoclinic	orthorhombic
space group	$P2_1/c$	*Pnma*
cell dimens		
a/Å	7.784 (3)	5.950 (3)
b/Å	12.642 (5)	11.592 (3)
c/Å	14.728 (4)	15.122 (3)
β/deg	119.98 (2)	
V/Å^3	1255.4 (7)	1043 (1)
Z	4	4
formula mass/amu	471.4	443.4
density (calc)/Mg m^{-3}	2.494	2.823
abs coeff/mm^{-1}	10.653	12.817
F(000)	872	808
diffractometer	Nicolet R3m/V	Rigaku AFC6S
radiation	Mo Kα	Mo Kα
wavelength/Å	0.710 73	0.710 69
temp/K	293	296
2θ(max)/deg	50	50
scan type	2θ–θ	ω–2θ
index range	$-9 \le h \le 9, -15 \le k \le 0, -19 \le l \le 9$	$0 \le h \le 7, 0 \le k \le 14, 0 \le l \le 18$
scan speed/deg min^{-1} (in ω)	3–14.5	4.0
scan range (ω)/deg	0.60 + Kα separation	1.05 + 0.30 tan θ[a]
no. of rflns measd	2471	1109
no. of indep rflns	2221 (R_{int} = 5.63%)	1109
no. of obsd rflns	1597 ($F > 4\sigma(F)$)	634 ($F > 6\sigma(F)$)
corrections applied	Lorentz–polarization, empirical abs (ψ scans)	
soln	Patterson	
refinement	full-matrix least squares	
quantity minimized	$\sum w(F_o - F_c)^2$	
H atoms	Riding model, fixed isotropic U	calcd with fixed isotropic U
weighting scheme	$w^{-1} = \sigma^2(F) + 0.0007F^2$	$4F_o^2/\sigma^2(F_o^2)$
final R (obsd data)	R = 4.56, R_w = 5.01	R = 3.2, R_w = 3.3
goodness of fit	1.24	1.10
largest Δ/σ	0.019	0.03
data-to-param ratio	9.2	7.5
no. of variables	174	85
largest diff peak/e Å^{-3}	1.67	0.90
largest diff hole/e Å^{-3}	−1.73	−1.11

[a] Weak reflections ($I < 10\sigma(I)$) were rescanned once or twice.

Table III. Atomic Coordinates (×10^4) of Non-Hydrogen Atoms and Equivalent Isotropic Displacement Coefficients (Å^2 × 10^3) for $CpIr(C_2H_4)(\eta^2\text{-}C_6F_6)$

	x	y	z	U(eq)[a]
Ir(1)	2316 (1)	1562 (1)	3759 (1)	40 (1)
C(1)	1923 (34)	−7 (15)	4111 (17)	96 (15)
C(2)	71 (31)	392 (15)	3337 (17)	88 (12)
C(3)	1147 (20)	2344 (12)	4564 (11)	47 (7)
F(3)	−352 (13)	1841 (8)	4676 (8)	86 (6)
C(4)	3173 (20)	1977 (12)	5295 (11)	51 (7)
F(4)	3372 (16)	1202 (7)	6003 (7)	78 (5)
C(5)	4630 (22)	2783 (14)	5838 (11)	57 (8)
F(5)	6462 (13)	2500 (11)	6510 (8)	103 (6)
C(6)	4176 (25)	3816 (15)	5675 (13)	66 (9)
F(6)	5491 (16)	4564 (9)	6132 (9)	101 (7)
C(7)	2187 (30)	4120 (14)	4933 (14)	67 (10)
F(7)	1889 (18)	5187 (8)	4760 (9)	96 (7)
C(8)	727 (22)	3439 (13)	4397 (12)	57 (7)
F(8)	−1062 (15)	3756 (9)	3738 (8)	95 (6)
C(10)	3345 (39)	2916 (11)	3167 (17)	108 (18)
C(11)	1672	2439	2306	102 (14)
C(12)	2172	1377	2224	122 (20)
C(13)	4155	1197	3035	151 (28)
C(14)	4879	2148	3617	130 (16)

[a] Equivalent isotropic U defined as one-third of the trace of the orthogonalized U_{ij} tensor.

atoms were refined anisotropically. Hydrogen atoms were then included in calculated positions with a common isotropic temperature factor for those of the cyclopentadienyl ring and a separate factor for those of the ethene group. Neutral atom scattering factors were employed, and anomalous dispersion effects were included in F_{calc}.[10a] The final refinement of the 174 variable parameters converged with R = 0.0456 and R_w = 0.0501. The largest peaks in the final difference map occurred at close proximity to the iridium atom. Final positional parameters are listed in Table III and selected bond lengths and angles in Table IV. Full crystallographic data and a packing diagram are given in the supplementary material (Tables VIII–XII and Figure 5). Plots were generated by the SHELXTL-PLUS package[9a] and the TEXSAN software.[9b] All calculations were carried out with the SHELXTL-PLUS software package.[9a]

Table IV. Selected Bond Lengths (Å) and Angles (deg) for $CpIr(C_2H_4)(\eta^2\text{-}C_6F_6)$

Ir(1)–C(1)	2.11 (2)	Ir(1)–C(2)	2.13 (2)
Ir(1)–C(3)	2.07 (2)	Ir(1)–C(4)	2.08 (2)
Ir(1)–C(10)	2.24 (2)	Ir(1)–C(11)	2.23 (2)
Ir(1)–C(12)	2.22 (3)	Ir(1)–C(13)	2.22 (3)
Ir(1)–C(14)	2.23 (3)	C(1)–C(2)	1.41 (3)
C(3)–F(3)	1.41 (2)	C(3)–C(4)	1.47 (2)
C(3)–C(6)	1.42 (2)	C(4)–F(4)	1.38 (2)
C(4)–C(5)	1.43 (2)	C(5)–F(5)	1.32 (2)
C(5)–C(6)	1.34 (3)	C(6)–F(6)	1.31 (2)
C(6)–C(7)	1.43 (2)	C(7)–F(7)	1.37 (2)
C(7)–C(8)	1.33 (2)	C(8)–F(8)	1.30 (2)
C(1)–Ir(1)–C(2)	38.9 (7)	C(1)–Ir(1)–C(3)	98.6 (9)
C(2)–Ir(1)–C(3)	88.1 (8)	C(1)–Ir(1)–C(4)	88.7 (8)
C(2)–Ir(1)–C(4)	105.3 (8)	C(3)–Ir(1)–C(4)	41.5 (5)
Ir(1)–C(1)–C(2)	71 (1)	Ir(1)–C(2)–C(1)	70 (1)
Ir(1)–C(3)–F(3)	119 (1)	Ir(1)–C(3)–C(4)	70 (1)
F(3)–C(3)–C(4)	115 (1)	Ir(1)–C(3)–C(8)	120 (1)
F(3)–C(3)–C(8)	109 (1)	C(4)–C(3)–C(8)	120 (1)
Ir(1)–C(4)–C(3)	68.9 (9)	Ir(1)–C(4)–F(4)	119 (1)
C(3)–C(4)–F(4)	117 (1)	Ir(1)–C(4)–C(5)	121 (1)
C(3)–C(4)–C(5)	116 (1)	F(4)–C(4)–C(5)	109 (1)
C(4)–C(5)–F(5)	119 (2)	C(4)–C(5)–C(6)	122 (1)
F(5)–C(5)–C(6)	119 (2)	C(5)–C(6)–F(6)	123 (1)
C(5)–C(6)–C(7)	119 (2)	F(6)–C(6)–C(7)	118 (2)
C(6)–C(7)–F(7)	115 (2)	C(6)–C(7)–C(8)	124 (2)
F(7)–C(7)–C(8)	121 (2)	C(3)–C(8)–C(7)	119 (1)
C(3)–C(8)–F(8)	120 (1)	C(7)–C(8)–F(8)	122 (2)

Table V. Atomic Coordinates (×10^4) of Non-Hydrogen Atoms and Equivalent Isotropic Displacement Coefficients (Å^2 × 10^3) for $CpIr(\eta^4\text{-}C_6F_6)$

atom	x	y	z	U(eq)
Ir(1)	1821 (1)	2500	205 (1)	34 (1)
F(1)	−2237 (11)	3732 (7)	−708 (4)	54 (5)
F(2)	2090 (14)	4741 (6)	−814 (4)	59 (5)
F(3)	3911 (12)	3740 (8)	−2307 (4)	70 (6)
C(1)	−342 (19)	3107 (10)	−780 (7)	39 (7)
C(2)	1869 (25)	3584 (11)	−909 (7)	43 (8)
C(3)	3255 (22)	3057 (11)	−1632 (6)	46 (7)
C(4)	3414 (35)	1541 (15)	1278 (9)	73 (13)
C(5)	1350 (27)	1920 (16)	1605 (8)	89 (12)
C(6)	4716 (33)	2500	1092 (12)	80 (17)

Crystal Structure of $CpIr(\eta^4\text{-}C_6F_6)$. Diffraction measurements on a crystal of $CpIr(\eta^4\text{-}C_6F_6)$ were made on a Rigaku AFC6S diffractometer with graphite-monochromated Mo Kα radiation. Unit cell dimensions were determined by least-squares refinement of 25 reflections in the range $12.89 < 2\theta < 21.89°$ found in a random search. The data were corrected for absorption as described above, resulting in transmission factors ranging from 0.62 to 1.0. Further data collection parameters are contained in Table II. The structure was solved by a combination of the Patterson method, to locate the iridium atom, and direct methods, to find all other non-hydrogen atoms. Non-hydrogen atoms were refined anisotropically. Hydrogen atoms were included in calculated positions with isotropic temperature factors fixed at 1.2 times those of adjoining carbon atoms. Neutral atom scattering factors were used,[10a] and anomalous dispersion effects were included in F_{calc}.[10b] The final refinement of the 85 parameters converged with R = 0.032 and R_w = 0.033. Once more, the largest peaks in the difference map occurred close to the iridium atom. Atomic coordinates and thermal parameters are listed in Table V and selected

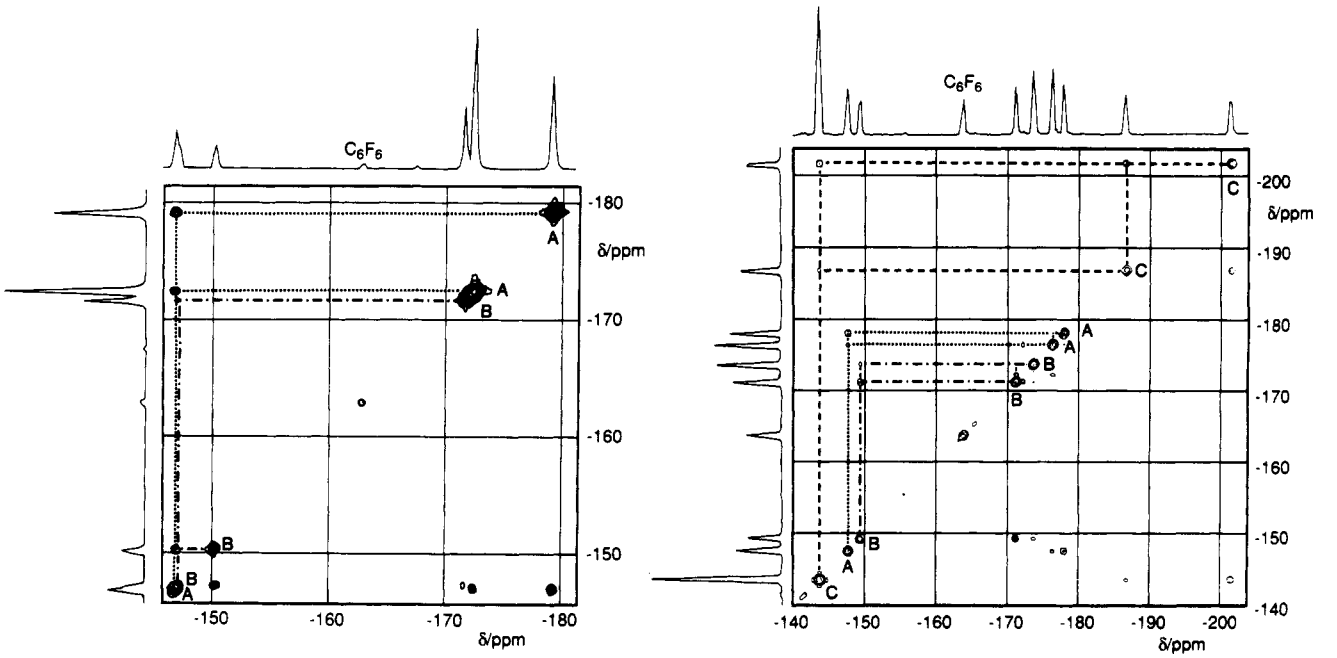

(a) (b)

Figure 1. ^{19}F–^{19}F COSY spectra of (a) $CpIr(C_2H_4)(\eta^2\text{-}C_6F_6)$ in toluene-d_8 and (b) a mixture of $Cp^*Ir(C_2H_4)(\eta^2\text{-}C_6F_6)$ and $Cp^*Ir(\eta^4\text{-}C_6F_6)$.

Table VI. Selected Bond Lengths (Å) and Angles (deg) for $CpIr(\eta^4\text{-}C_6F_6)$

Ir(1)–C(1)	2.09 (1)	C(1)–C(1′)	1.41 (2)
Ir(1)–C(2)	2.10 (1)	C(1)–C(2)	1.44 (2)
Ir(1)–C(4)	2.18 (1)	C(2)–C(3)	1.50 (2)
Ir(1)–C(5)	2.24 (1)	C(3)–C(3′)	1.29 (3)
Ir(1)–C(6)	2.18 (2)	C(4)–C(5)	1.39 (2)
F(1)–C(1)	1.34 (1)	C(4)–C(6)	1.38 (2)
F(2)–C(2)	1.36 (1)	C(5)–C(5′)	1.34 (4)
F(3)–C(3)	1.35 (1)		
C(1)–Ir(1)–C(1)	39.3 (6)	Ir(1)–C(2)–F(2)	120.5 (8)
C(1)–Ir(1)–C(2)	40.2 (5)	Ir(1)–C(2)–C(1)	69.5 (6)
C(1)–Ir(1)–C(2′)	68.8 (5)	Ir(1)–C(2)–C(3)	110.4 (8)
C(2)–Ir(1)–C(2)	73.4 (7)	F(2)–C(2)–C(1)	117 (1)
Ir(1)–C(1)–F(1)	129.8 (7)	F(2)–C(2)–C(3)	115 (1)
Ir(1)–C(1)–C(1)	70.3 (3)	C(1)–C(2)–C(3)	116 (1)
F(1)–C(1)–C(1)	122.6 (6)	F(3)–C(3)–C(2)	118 (1)
F(1)–C(1)–C(2)	125 (1)	F(3)–C(3)–C(3)	125.9 (6)
C(1)–C(1)–C(2)	112.6 (7)	C(2)–C(3)–C(3)	114.0 (7)

bond lengths and angles in Table VI. Full crystallographic data and a packing diagram are given in the supplementary material (Tables XIV–XVIII and Figure 6). All calculations and graphics processes were carried out with the TEXSAN software package.[9b]

Results

Synthesis of C_6F_6 Complexes. Irradiation of a solution of $CpIr(C_2H_4)_2$ ($\lambda > 315$ nm) generates four CpIr products with an overall conversion of about 50% after 16 h of photolysis. Two materials may be obtained by sublimation and chromatography from this mixture. The first of these is revealed to be $CpIr(C_2H_4)(\eta^2\text{-}C_6F_6)$ by a combination of ^{19}F and ^1H NMR spectroscopy together with mass spectrometry and is present in two isomeric forms (see below). The second material is identified similarly as $CpIr(\eta^4\text{-}C_6F_6)$. Both assignments have been confirmed crystallographically. The smallest of the original CpIr product resonances (δ 4.84 in toluene-d_8) has not yet been identified. When a sample containing $CpIr(C_2H_4)(\eta^2\text{-}C_6F_6)$ and $CpIr(\eta^4\text{-}C_6F_6)$ in a ratio of 20:1 is redissolved in C_6F_6 and irradiated again ($\lambda > 315$ nm, 24 h), the proportion of $CpIr(\eta^4\text{-}C_6F_6)$ increased dramatically, so that the two products are present in a ratio of 2.5:1. This evidence establishes that we are observing the reactions given in eq 1.

$$CpIr(C_2H_4)_2 \xrightarrow{h\nu,\ C_6F_6} CpIr(C_2H_4)(\eta^2\text{-}C_6F_6) \xrightarrow{h\nu} CpIr(\eta^4\text{-}C_6F_6) \quad (1)$$

NMR Spectroscopy of $CpIr(C_2H_4)(\eta^2\text{-}C_6F_6)$. Proton NMR spectra reveal that $CpIr(C_2H_4)(\eta^2\text{-}C_6F_6)$ is present in solution in two isomeric forms with widely different parameters (Table I). Even when pure crystalline compound is redissolved, both isomers are observed. The major isomer has a Cp resonance at δ 4.2, shifted 0.7 ppm upfield from that for $CpIr(C_2H_4)_2$, and relatively close resonances for the two ethene multiplets (δ 2.72 and 2.30). The minor isomer has a normal Cp resonance (δ 4.72) and widely spaced ethene resonances (δ 2.46 and 0.24). The $^{13}C\{^1H\}$ NMR resonance for coordinated ethene for the major isomer is a doublet (J_{CF} = 16.5 Hz both at 75 and at 23 MHz), implying that there may be a C–H···F interaction as in A (see crystallographic section). The corresponding resonance for the minor isomer is a singlet. Each isomer exhibits three multiplets in the ^{19}F NMR spectrum, indicating a rigid structure with three pairs of equivalent fluorine atoms, similar to that of $CpRh(PMe_3)(\eta^2\text{-}C_6F_6)$. Their connectivity is established by ^{19}F–^{19}F COSY (Figure 1a). The minor isomer is probably the rotamer formed by internal rotation about the Ir–C_6F_6 bond.

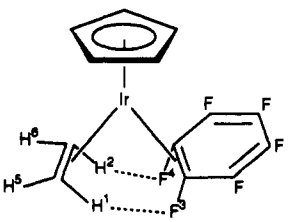

major isomer A

Following the observation of ^{19}F coupling to the ethene carbon atoms, we undertook selective $^1H\{^{19}F\}$ decoupling experiments for the major isomer. By these means, we

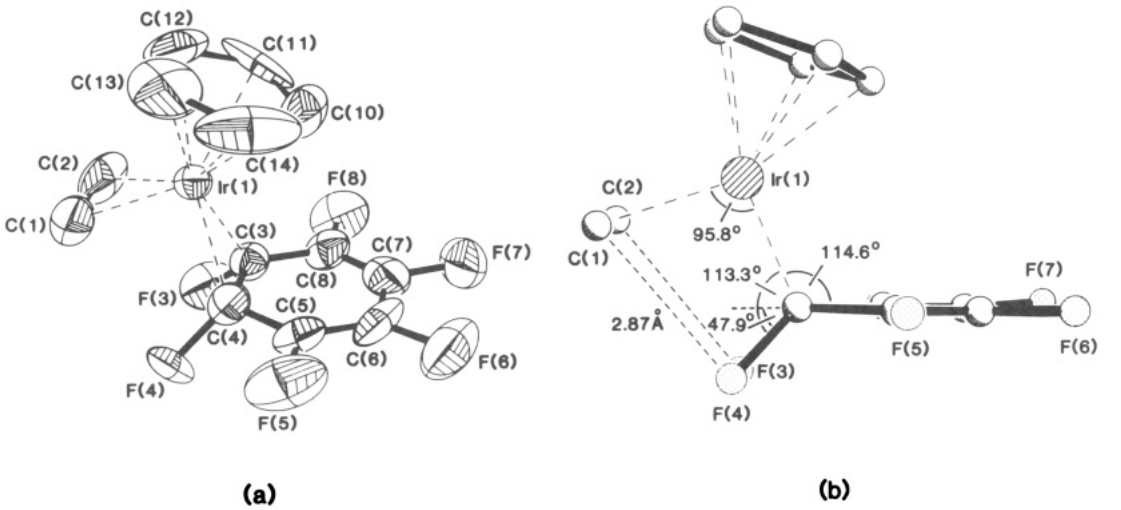

Figure 2. Two views of $CpIr(C_2H_4)(\eta^2\text{-}C_6F_6)$: (a) ORTEP plot; (b) PLUTO plot showing the C_6F_6 ring edge-on.

established that the ^{19}F resonance at δ 179.1 is coupled to both sets of ethene protons. The other ^{19}F resonances are not coupled to the ethene protons. The ethene resonances were simulated in two stages, first without ^{19}F coupling and then with ^{19}F coupling (Table I).

The ratio of major to minor isomers in $CpIr(C_2H_4)(\eta^2\text{-}C_6F_6)$ remains 2.7 ± 0.1 in toluene-d_8 over the temperature range 200–293 K. We therefore looked to other means to establish whether the isomers are at equilibrium. When the solvent is changed, the isomer ratio does indeed change (CD_3CN ratio 4.8, C_6D_{12} ratio 2.2), returning to the original ratio when the sample is redissolved in toluene. Irradiation of the Cp protons of one isomer failed to induce magnetization transfer to the other isomer at room temperature. Since thermal decomposition sets in below 60 °C, we did not carry out magnetization transfer experiments at higher temperatures. We conclude that the two isomers are at equilibrium but that the rate of interconversion is slow compared to the relaxation times. T_1 is measured to be 26.2 s for the major isomer and 23.5 s for the minor isomer by the inversion-recovery method.

NMR Spectroscopy of $CpIr(\eta^4\text{-}C_6F_6)$. The ^1H NMR spectrum of $CpIr(\eta^4\text{-}C_6F_6)$ shows one singlet for the Cp protons at δ 4.56. The ^{19}F spectrum shows three multiplets, consistent with a formulation as a complex of η^4-hexafluorobenzene but not as a complex of η^4-hexafluoro(Dewar benzene).[11]

Photolysis of $Cp^*Ir(C_2H_4)_2$. The photolysis of $Cp^*Ir(C_2H_4)_2$ proceeds in a fashion similar to that for the Cp complexes. However, shorter photolysis times could be used, probably because of a reduction in the level of photodecomposition. Consequently, we could also decrease the photolysis wavelength to $\lambda > 285$ nm.

After 3 h of photolysis, there was already 82% conversion to products with an 18:50:31 $Cp^*Ir(C_2H_4)_2$:$Cp^*Ir(C_2H_4)(\eta^2\text{-}C_6F_6)$:$Cp^*Ir(\eta^4\text{-}C_6F_6)$ distribution. After 23 h of photolysis there is >95% conversion to $Cp^*Ir(\eta^4\text{-}C_6F_6)$. The characterization of these complexes follows the same pattern as for the Cp analogues. Since there is no overlap between the different ^{19}F peaks, all the connections may be seen in a single COSY spectrum of a reaction mixture (Figure 1b). There are again two isomers of the monosubstitution product, $Cp^*Ir(C_2H_4)(\eta^2\text{-}C_6F_6)$, with Cp* resonances at δ 1.71 and 1.50; they are present in a ratio of 1.2:1.

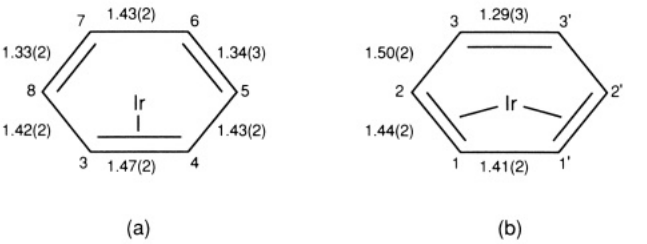

Figure 3. Bond lengths (Å) of the C_6F_6 ring in (a) $CpIr(C_2H_4)(\eta^2\text{-}C_6F_6)$ and (b) $CpIr(\eta^4\text{-}C_6F_6)$.

Crystal and Molecular Structure of $CpIr(C_2H_4)(\eta^2\text{-}C_6F_6)$. The primary photoproduct, $CpIr(C_2H_4)(\eta^2\text{-}C_6F_6)$, crystallizes in space group $P2_1/c$ with no crystallographically imposed symmetry. However, the molecular structure (Figure 2, Table IV) shows an $Ir(C_2H_4)(\eta^2\text{-}C_6F_6)$ moiety with approximate mirror symmetry. The $CpIr(C_2H_4)$ unit exhibits no unusual features. The mean iridium–carbon distances are 2.12 (2) Å for the coordinated ethene and 2.08 (2) Å for the hexafluorobenzene. The bond angle subtended by the ethene and hexafluorobenzene ligands at iridium is 95.8° (measured to the midpoints of the C=C vectors), similar to that for other $CpM(C_2H_4)L$ complexes.[2,12] The CC vectors of the coordinated C_2H_4 and C_6F_6 are only 3.2° from parallel. The most striking feature of the structure is the planar C_6F_4 unit (mean deviation from plane 0.0160 Å) bonded through C(3) and C(4) and tipped toward the cyclopentadienyl group. The fluorines on the bonding carbons (F(3) and F(4)) are tipped out of the plane, so that the dihedral angle between the C(3)F(3)C(4)F(4) plane and the C_6 plane is 47.9°. These two fluorine atoms lie close to the ethene carbons (C(1)···F(4) = 2.87 (2) Å, C(2)···F(3) = 2.83 (2) Å), well within the sum of the carbon and fluorine van der Waals radii (3.17 Å).[13] The C_6 skeleton of the C_6F_6 ligand is considerably distorted (Figure 3a). The coordinated C–C bond has a length of 1.47 (2) Å, increased significantly compared to 1.394 (7) Å for free C_6F_6.[14a] The

(11) Cooke, D. J.; Green, M.; Mayne, N.; Stone, F. G. A. *J. Chem. Soc. A* **1968**, 1771. Booth, B. L.; Haszeldine, R. N.; Tucker, N. I. *J. Chem. Soc., Dalton Trans.* **1975**, 1439.

(12) Ryan, R. R.; Eller, P. G.; Kubas, G. J. *Inorg. Chem.* **1976**, *15*, 797. Mlekuz, M.; Bougeard, P.; Sayer, B. G.; McGlinchey, M. J.; Rodgers, C. A.; Churchill, J. W.; Zeller, J.; Kanz, S. W.; Albright, T. A. *Organometallics* **1986**, *5*, 1656.

(13) In the structure of $CpRh(PMe_3)(\eta^2\text{-}C_6F_6)$, the two fluorines bound to the coordinated carbons also lie within hydrogen-bonding distance of the phosphine methyls (C···F = 2.77 Å).

(14) (a) Almenningen, A.; Bastiansen, O.; Seip, R.; Seip, H. M. *Acta Chem. Scand.* **1964**, *18*, 2115. (b) Calculated with value of r(CC) for C_2F_4 more precise than was available at the time of ref 2: Carlos, J. L.; Karl, R. R.; Bauer, S. H. *J. Chem. Soc., Faraday Trans. 2* **1974**, *70*, 177.

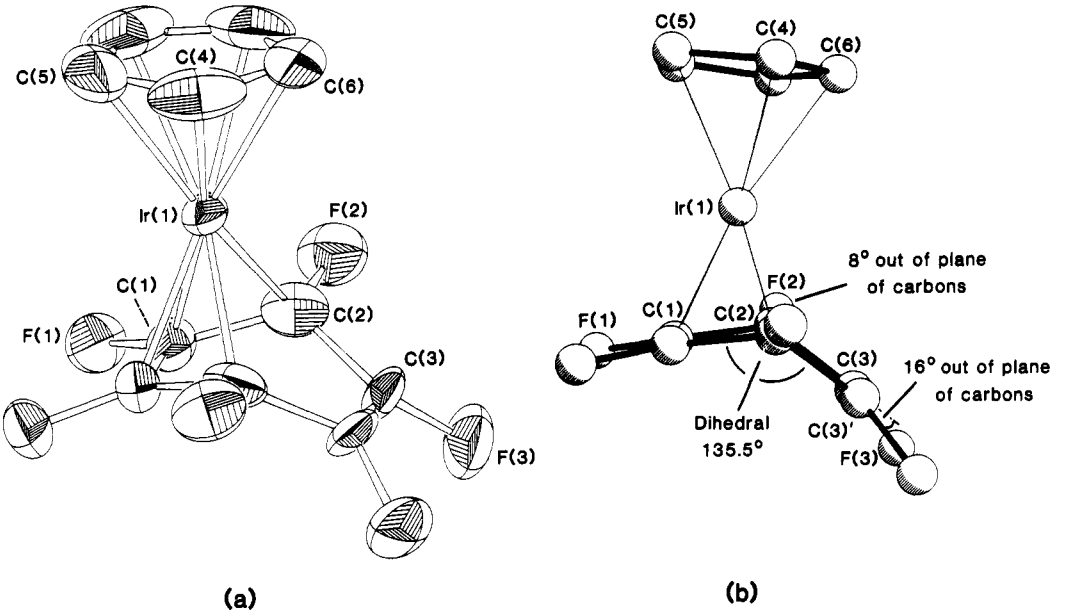

Figure 4. Two views of $CpIr(\eta^4\text{-}C_6F_6)$: (a) ORTEP plot; (b) PLUTO plot showing the C_6F_6 ring edge-on.

C(5)C(6)C(7)C(8) unit resembles a free diene with a short, medium, short pattern (mean of C(5)–C(6) and C(7)–C(8) 1.34 (3) Å, C(6)–C(7) = 1.43 (2) Å). The remaining two C–C bonds have a mean length of 1.42 (2) Å. Thus, the difference between the shortest and the longest C–C distances in the C_6F_6 ring is 0.14 Å, more than 6 times the mean esd.

The above considerations confirm that the C_6F_6 ligand resembles a coordinated alkene in geometry. Indeed, the vector from the midpoint of C(3)–C(4) to Ir approximately bisects the angle between the C(3)C(4)F(3)F(4) plane and the plane of the C_6 ring (Figure 2b). It seemed appropriate, therefore, to analyze the angles at the coordinated C–C bond by the Ibers method for an alkene.[15] The values of the Ibers parameters are

α = 76.7° (angle between planes F(3)C(3)C(8) and F(4)C(4)C(5))

β = 53.2° (angle between plane F(3)C(3)C(8) and C(3)C(4))

β' = 50.3° (angle between plane F(4)C(4)C(5) and C(3)C(4))

γ = 133 (2)° (torsion F(4)C(4)C(3)C(8))

γ' = −132 (2)° (torsion F(3)C(3)C(4)C(5))

δ = 113 (1)° (torsion IrC(4)C(3)F(3))

δ' = −114 (1)° (torsion IrC(3)C(4)F(4))

These values are remarkably close to those for the C_2F_4 unit of $CpRh(C_2F_4)(C_2H_4)$ of α = 74.3°, β = 52.8°, γ = 131.4°, and δ = 114.3°.[2a] Thus, the C_6F_6 ligand of $CpIr(C_2H_4)(\eta^2\text{-}C_6F_6)$ closely resembles the C_2F_4 ligand of $CpRh(C_2F_4)(C_2H_4)$. The C–C distances of the fluorinated ligands in these two complexes differ significantly (1.471 (17) and 1.405 (7) Å), but their extensions relative to the free ligands are similar (0.077 (18) and 0.094 (8) Å, respectively).[14]

Crystal and Molecular Structure of $CpIr(\eta^4\text{-}C_6F_6)$. The crystal structure of $CpIr(\eta^4\text{-}C_6F_6)$ reveals that iridium is coordinated to a diene-like C_4F_4 unit with the remaining C_2F_2 unit folded out of the way of the metal (Table VI, Figure 4). There is a crystallographic mirror plane (space group *Pnma*) at right angles to the fold of the ligand. The four bonded Ir–C distances are essentially equal at 2.09 (1) and 2.10 (1) Å. The lengths of the coordinated C–C bonds of the C_6F_6 are almost equal at 1.41 (2) and 1.44 (2) Å, while the uncoordinated double bond is significantly shorter at 1.29 (3) Å (Figure 3b). The folding angle of the C_6F_6 ring is 135.5° (i.e. the dihedral angle between the planes C(1)C(1′)C(2)C(2′) and C(2)C(2′)C(3)C(3′)). The C–F vectors deviate from the planes of the C_6 ring. Thus, the dihedral angles between the plane normals are

C(1)C(1′)F(1)F(1′) and C(1)C(1′)C(2)C(2′) τ = 2.9°

C(3)C(3′)F(3)F(3′) and C(2)C(2′)C(3)C(3′) τ = 16.2°

The C–F bonds in the mirror plane are tipped toward the metal so that C(2)–C(2′)–F(2) = 8.2°. The angle between the normals to the plane of the coordinated carbons of the C_6F_6 ligand and that of the Cp ligand is 12.9°.

Discussion

There has been considerable recent interest in partial coordination of arenes. Notable examples include the work of the groups of Bianchini,[16] Cooper,[17] Jonas,[18] Jones,[19] and Taube.[20] The evidence presented above demonstrates that the ethene ligands of $(\eta^5\text{-}C_5R_5)Ir(C_2H_4)_2$ (R = H, Me) are replaced successively on photolysis in C_6F_6. In contrast to the photolysis of $Cp^*Rh(PMe_3)(C_2H_4)$ and $CpIr(PMe_3)H_2$,[7,21] no C–F activation occurs. The sequential photosubstitution also contrasts with the effect of photolysis in the presence of triphenylphosphine, which gener-

(15) Ittel, S. D.; Ibers, J. A. *Adv. Organomet. Chem.* **1976**, *14*, 33.

(16) Bianchini, C.; Caulton, K. G.; Chardon, C.; Eisenstein, O.; Folting, K.; Johnson, J. J.; Meli, A.; Peruzzini, M.; Rauscher, D. J.; Streib, W. E.; Vizza, F. *J. Am. Chem. Soc.* **1991**, *113*, 5127.

(17) Lees, S.; Cooper, N. J. *J. Am. Chem. Soc.* **1991**, *113*, 716. Leong, V. S.; Cooper, N. J. *J. Am. Chem. Soc.* **1988**, *110*, 2644. Corella, J. A.; Cooper, N. J. *J. Am. Chem. Soc.* **1990**, *112*, 2833.

(18) Jonas, K.; Wiskamp, V.; Tsay, Y.-H.; Krüger, C. *J. Am. Chem. Soc.* **1983**, *105*, 5480. Jonas, K. *Pure Appl. Chem.* **1990**, *62*, 1169; *J. Organomet. Chem.* **1990**, *400*, 165.

(19) Jones, W. D.; Dong, L. *J. Am. Chem. Soc.* **1989**, *111*, 8722. Jones, W. D.; Feher, F. J. *Acc. Chem. Res.* **1989**, *22*, 91.

(20) Harman, W. D.; Taube, H. *J. Am. Chem. Soc.* **1987**, *109*, 1883; **1988**, *110*, 7906; **1988**, *110*, 7555. Harman, W. D.; Sekini, M.; Taube, H. *J. Am. Chem. Soc.* **1988**, *110*, 5725. Harman, W. D.; Taube, H. *Inorg. Chem.* **1987**, *26*, 2917.

(21) Bell, T. W.; Partridge, M. G.; Perutz, R. N. Unpublished results. Haddleton, D. M.; Perutz, R. N. *J. Chem. Soc., Chem. Commun.* **1986**, 1734.

ates a vinyl hydride, $CpIr(PPh_3)(C_2H_3)H$, via the photosubstitution product $CpIr(PPh_3)(C_2H_4)$.[21] Low-temperature irradiation of $CpIr(C_2H_4)_2$ in solid argon or solid toluene does not dissociate ethene but results in isomerization to the vinyl hydride, $CpIr(C_2H_4)(C_2H_3)H$, a reaction thought to proceed via a $CpIr(C_2H_4)\cdots(C_2H_4)$ cage complex.

The first product of reaction with C_6F_6, $(\eta^5\text{-}C_5R_5)Ir(C_2H_4)(\eta^2\text{-}C_6F_6)$, is present in two isomeric forms. The crystal structure of the C_5H_5 complex shows the C_6F_4 unit tipped toward the Cp and reveals close contacts between the ethene hydrogens and the two fluorines bound to the coordinated carbons. Since the major isomer in solution shows strong coupling between the ethene nuclei and the fluorine nuclei, we assign this as the isomer with intramolecular interaction (A). The minor isomer is likely to be the rotamer with the C_6F_4 unit tipped toward the ethene (B in eq 2). In this isomer there is no coupling between the ethene carbons and the fluorine nuclei.

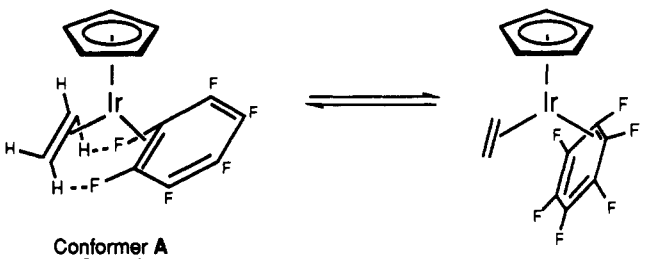

(2)

R = H: K = 0.21 (CD_3CN), 0.37 (toluene-d_8), 0.45 (C_6D_{12})

R = Me: K = 0.83 or 1.2 (toluene-d_8)

A model of the structure of isomer B was constructed with molecular graphics starting from the crystallographic coordinates and rotating the C_6F_6 unit by 180° about the vector joining Ir to the midpoint of the coordinated C–C bond of C_6F_6. The model showed no close contacts between fluorines and hydrogens, suggesting that conformer B is not sterically congested. The effect of rotation about the Ir–C_6F_6 bond on noncovalent interactions was modeled by molecular mechanics calculations with the aid of the QUANTA/CHARM package.[22] Potential minima were revealed corresponding to the crystallographic geometry and to that proposed for conformer B, but no other minima were located. This evidence provides considerable support for the assignment of the minor isomer as conformer B.

The two isomers show notable differences in the ^1H chemical shifts of the Cp and ethene protons, and in the ^{19}F shift of the fluorine bound to the coordinated carbon. When the C_5H_5 ligand is replaced by C_5Me_5, the isomer ratio is close to unity, but the isomers have not been specifically assigned. The rate of rotation is so slow that no magnetization transfer is observed at ambient temperature. There is no rotation of the C_2H_4 at ambient temperature (cf. the very high barrier for $CpIr(C_2H_4)_2$).[23]

The structure of $CpIr(C_2H_4)(\eta^2\text{-}C_6F_6)$ demonstrates that C_6F_6 is coordinated very much like a fluoroalkene such as C_2F_4, leaving a free diene unit. There are few structures available for mononuclear η^2-arene complexes which may be compared to this one. The most closely related is $CpRh(PMe_3)(\eta^2\text{-}C_6F_6)$, which exhibits a similar bending of two C–F bonds out of the C_6F_4 plane but shows a somewhat different distortion of the C–C distances.[6] The d^{10} complex $Pt(PEt_3)_2[\eta^2\text{-}C_6(CF_3)_6]$ has a pattern of C–C bond lengths[4] similar to that for $CpIr(C_2H_4)(\eta^2\text{-}C_6F_6)$. Other η^2-arene complexes are constrained to appreciably different geometries by the use of a fused polycyclic arene, as in $Cp^*Rh(PMe_3)(\eta^2$-phenanthrene),[18,19,24] or by the coordination of a second metal to the arene, as in $[Cp^*Re(CO)_2]_2(\mu\text{-}\eta^2\text{:}\eta^2\text{-}C_6H_6)$ and $[Cp^*Ru]_2(\mu\text{-}PPh_2)(\mu\text{-}H)(\mu\text{-}\eta^2\text{:}\eta^2\text{-}C_6H_6)$.[25,26]

Table VII. Geometric Parameters of η^4-Arene Complexes

complex	r(C=C)/Å coord	r(C=C)/Å uncoord	dihedral fold of carbon planes/deg	ref
$CpIr(\eta^4\text{-}C_6F_6)$	1.44 (2) 1.41 (2) 1.44 (2)	1.29 (3)	135.5	this work
$CpRh[\eta^4\text{-}C_6(CF_3)_6]$	1.53 (2) 1.42 (2) 1.48 (2)	1.31 (2)	132.1	5
$(\eta^6\text{-}C_6Me_6)Ru(\eta^4\text{-}C_6Me_6)$	1.42 (1) 1.41 (1) 1.48 (1)	1.34 (1)	137.2	29
$[(pp_3)Ir(\eta^4\text{-}C_6H)_6]^+$	1.49 (3) 1.37 (3) 1.49 (3)	1.36 (3)	134.8	16
$(OC)_3Fe[\eta^4\text{-}C_6Me_4(CF_3)_2]$	1.462 (5) 1.410 (5) 1.453 (4)	1.352 (5)	136.0	30
$LRh[\eta^4\text{-}C_6(CF_3)_6]^a$	1.49 (1) 1.40 (1) 1.48 (1)	1.38 (2)	138	31

[a] L = $C_9H_7F_6O_2$.

There are several arguments which show that the interaction between C_2H_4 and C_6F_6 in conformer A leads to a stabilization. (i) The C–H···F distance in the crystal is well within the sum of the van der Waals radii. (ii) NMR spectroscopy reveals C–H···F coupling in solution. The requirement for such "through-space" coupling is close approach of the coupled proton and fluorine nuclei,[27] enabling spin correlation to occur. (iii) The conformer A is preferred in the case of the Cp complex and equal in population in the Cp* complex. Conformer B has been shown to be free of steric constraints; thus, it follows that the molecule is not forced into the geometry of conformer A in solution. Such interactions have been observed previously in organometallic fluorine compounds, most notably in $Cp_2Ru_2(CO)[CF_2{=}CF(CF_3)](\mu\text{-}CO)(\mu\text{-}CH_2)$.[28] Some authors refer to such interactions as hydrogen bonds.[28]

The second photochemical step results in coordination of a second double bond of hexafluorobenzene, giving $(\eta^5\text{-}C_5R_5)Ir(\eta^4\text{-}C_6F_6)$. The structure of the Cp complex shows that the C_6F_6 ligand folds so as to retain four carbons close to the metal and two distant. In contrast to the $\eta^2\text{-}C_6F_6$ complex, the CF vectors are now close to the appropriate carbon planes. The principal geometric parameters of $CpIr(\eta^4\text{-}C_6F_6)$ are compared to those of other η^4-arene complexes in Table VII.[5,16,29-31] The dihedral angle of the ring is remarkably constant at ca. 135°, but

(22) Software provided by Polygen/Molecular Simulations.
(23) Szajek, L. P.; Lawson, R. J.; Shapley, J. R. *Organometallics* **1991**, *10*, 357.
(24) Brauer, J. D.; Krüger, C. *Inorg. Chem.* **1977**, *16*, 884.
(25) Van der Heiden, H.; Orpen, A. G.; Pasman, P. *J. Chem. Soc., Chem. Commun.* **1985**, 1576.
(26) Omori, H.; Suzuki, H.; Take, Y.; Moro-oka, Y. *Organometallics* **1989**, *8*, 2270.
(27) Hilton, J.; Sutcliffe, L. H. *Prog. NMR Spectrosc.* **1975**, *10*, 27.
(28) Howard, J. A. K.; Knox, S. A. R.; Terrill, N. J.; Yates, M. I. *J. Chem. Soc., Chem. Commun.* **1989**, 640.
(29) Huttner, G.; Lange, S. *Acta Crystallogr.* **1972**, *B28*, 2049.
(30) Bond, A.; Bottrill, M.; Green, M.; Welch, A. J. *J. Chem. Soc., Dalton Trans.* **1977**, 2373.
(31) Barlex, D. M.; Evans, J. A.; Kemmitt, R. D. W.; Russell, D. R. *J. Chem. Soc. D* **1971**, 331.

Scheme I. Photolysis of $(\eta^5\text{-}C_5R_5)Ir(C_2H_4)_2$ with C_6F_6

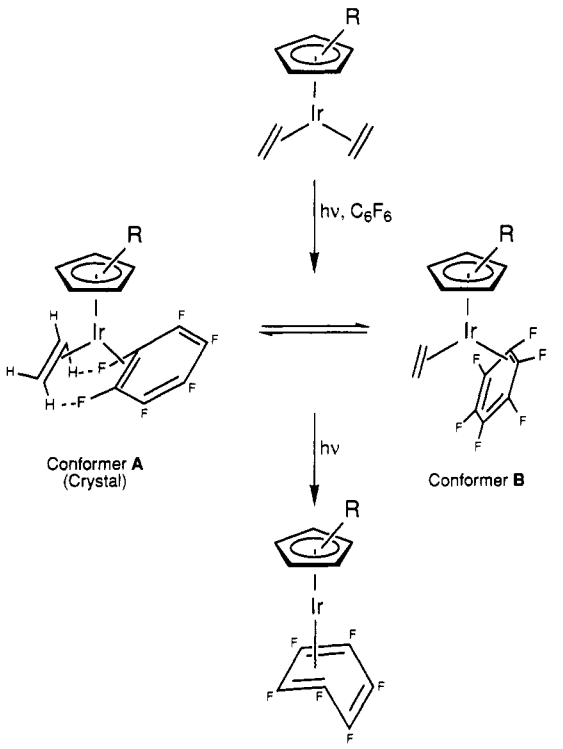

there are appreciable differences in the bond lengths of the coordinated carbon–carbon bonds. The dihedral angle is probably determined by the stereoelectronic demands of the η^4-coordination mode (i.e. the requirement to keep only four carbons within bonding distance of the metal). On the other hand, the C–C bond lengths reflect the different donor–acceptor properties of the metal fragment and arene.

Conclusions

The reaction of $(\eta^5\text{-}C_5R_5)Ir(C_2H_4)_2$ with hexafluorobenzene illustrates several general points (Scheme I).

(i) Hexafluorobenzene is a ligand capable of forming stable complexes in the η^2 and η^4 modes as well as the η^6 mode.[32] In doing so, its coordination behavior resembles those of fluoroalkenes and fluorodienes,[33] respectively.

(ii) Both the η^2 and η^4 coordination geometries require major distortions of bond lengths and angles within the C_6F_6 ligand which must require considerable reorganization energies. The η^2 geometry displaces two fluorines out of the C_6F_4 plane; the η^4 geometry folds the C_6 plane. The regular hexagon is distorted so as to leave an uncoordinated diene in the former and an uncoordinated alkene in the latter. In future experiments, we will investigate whether these units prove to react selectively.

(iii) It follows that either degenerate exchange of coordination positions or $\eta^2 \rightarrow \eta^4 \rightarrow \eta^6$ interconversion may require considerable geometric changes of the ligand and hence these are likely to be activated processes. The present complexes are stereochemically rigid, but Bianchini's recent $\eta^4\text{-}C_6H_6$ complex is fluxional.[16,34]

Acknowledgment. We are pleased to acknowledge the help of H.-J. Rohe and Dr. R. E. Hubbard in carrying out the molecular graphics investigations and that of Dr. E. Curzon of Bruker Spectrospin in measuring the $^1H\{^{19}F\}$ NMR spectra. We also appreciate extensive discussions with Dr. O. Eisenstein and financial support from the SERC, The Royal Society, British Gas, and the EC.

Supplementary Material Available: For the structures of $CpIr(C_2H_4)(\eta^2\text{-}C_6F_6)$ and $CpIr(\eta^4\text{-}C_6F_6)$, respectively, atomic coordinates (Tables VIII and XIV), anisotropic thermal parameters (Tables IX and XV), intramolecular distances (Tables X and XVI), intramolecular bond angles (Tables XI and XVII), least-squares planes (Tables XII and XVIII), and packing diagrams (Figures 5 and 6) (16 pages). Ordering information is given on any current masthead page.

OM9106894

(32) Middleton, R.; Hull, J. R.; Simpson, S. R.; Tomlinson, C. H.; Timms, P. L. *J. Chem. Soc., Dalton Trans.* **1973**, 120. Timms, P. L.; Turney, T. W. *Adv. Organomet. Chem.* **1977**, *15*, 53.

(33) Hitchcock, P. B.; McPartlin, M.; Mason, R. *J. Chem. Soc. D* **1969**, 1367. Doherty, N. M.; Ewels, B. E.; Hughes, R. P.; Samkoff, D. E.; Saunders, W. D.; Davis, R. E.; Laird, B. B. *Organometallics* **1985**, *4*, 1606. Carl, R. T.; Hughes, R. P.; Samkoff, D. E. *Organometallics* **1988**, *7*, 1625. Carl, R. T.; Hughes, R. P.; Rheingold, A. L.; Marder, T. B.; Taylor, N. J. *Organometallics* **1988**, *7*, 1613.

(34) $Cp^*Rh[\eta^4\text{-}C_6(CO_2Me)_6]$ is also fluxional at high temperature (T_c = 120 °C): Kang, J. W.; Childs, R. F.; Maitlis, P. M. *Inorg. Chem.* **1970**, 720. The ability to detect stereochemical nonrigidity depends on the chemical shift differences between the exchanging nuclei. The ^{19}F resonances of the C_6F_6 complexes are spread over a range of 24–61 ppm (=680–1720 Hz), far larger than any proton chemical shift differences.